Electrorheological Behavior of Main-Chain Liquid Crystal Polymers Dissolved in Nematic Solvents

Yen-Ching Chiang, Alex M. Jamieson,* M. Kawasumi, and V. Percec

Department of Macromolecular Science, Case Western Reserve University, Cleveland, Ohio 44106

Received August 29, 1996; Revised Manuscript Received January 23, 1997[⊗]

ABSTRACT: The Miesowicz viscosities η_c and η_b of dilute nematic solutions of the main-chain liquid crystal polymer (LCP) TPB*x*, in 4′-(pentyloxy)-4-cyanobiphenyl (5OCB) or 4′-pentyl-4-cyanobiphenyl (5CB) as nematic solvents, were measured by cone-and-plate rheometry in the presence and absence, respectively, of an external electric field. TPB*x* has a mesogenic group, 1-(4-hydroxy-4′-biphenyl)-2-(4-hydroxyphenyl)-butane, separated by flexible *n*-alkyl spacers of variable length *x*. Since for these solutions $\eta_c \gg \eta_b$, a pronounced electrorheological effect is observed, the viscosity with the field on being an order of magnitude larger than that with the field off. The intrinsic viscosity, $[\eta_c]$, of TPB10 in 5OCB, was found to follow a Mark−Houwink−Sakurada relationship, $[\eta_c] = KM^{\alpha}$, with $\alpha \approx 1.0$. Applying a theoretical description by Brochard, this result suggests that TPB10 behaves hydrodynamically in 5OCB like a free-draining random coil stretched along the director. Comparisons were made of $[\eta_c]$ and $[\eta_b]$ for TPB*x* and a hyperbranched LCP, TPD-b-8, based on a similar mesogen. From the ratio $[\eta_c]/[\eta_b]$, via the Brochard model, the ratio $(R_{\|}/R_{\perp})$ of the end-to-end distances of the LCP measured parallel and perpendicular to the nematic director were found to be ∼2−2.5 for TPB*x* and ∼1.45 for TPD-b-8, consistent with the expectation that the chain anisotropy of the branched species in the nematic state is smaller.

Introduction

The viscometric behavior of a nematic liquid crystal subjected to shear deformation depends strongly on the orientation of the nematic director relative to the direction of shear.[1] Here, we measure the Miesowicz viscosities of dilute nematic solutions of liquid crystalline polymers (LCPs) in low molar mass nematic solvents using cone-and-plate rheometry in the presence of a saturation electric field, applied perpendicular to the shear plane. With the electric field on, when the nematic has positive dielectric anisotropy, the nematic director is aligned parallel to the velocity gradient, and the viscosity measured is the Miesowicz viscosity η_c. With the electric field off, for a flow-aligning nematic, the nematic director orients nearly parallel to the shear flow direction, and the viscosity measured is close to the Miesowicz viscosity η_b. Previous work[2,3] has shown that lyotropic nematic solutions of stiff chain polymers exhibit a pronounced electrorheological (ER) effect which arises because the molecular axis of the extended chains aligns perpendicular to the flow direction when the field is on and rotates into the shear plane when the field is off. Here, we demonstrate that thermotropic solutions of main-chain LCPs, in low molar mass nematic solvents, also exhibit a pronounced ER effect. Again, the shear viscosity with the field on (η_c) is much larger than that with the field off (η_b). This ER effect occurs because the main-chain LCP adopts a stretched ellipsoidal conformation in the nematic solution state, the major axis of which aligns perpendicular to the shear direction when the field is on and near the shear direction when the field is off.

The magnitude of the increments in the viscosities, $\delta\eta_c$ and $\delta\eta_b$, where $\delta\eta = \eta_{solution} - \eta_{solvent}$, are determined by the size and shape of the dissolved LCP chain. We observe a strong molecular weight dependence of $\delta\eta_c$. These results are interpreted in terms of a theoretical description by Brochard,[4] by means of which $\delta\eta_c$ and $\delta\eta_b$ can be expressed in terms of $R_{\|}$ and $R_{\perp}$, i.e., the rms end-to-end distances of the polymer chain respectively parallel and perpendicular to the director. By comparing the ratio of $\delta\eta_c$ to $\delta\eta_b$, we can directly determine the ratio of $R_{\|}$ to $R_{\perp}$.

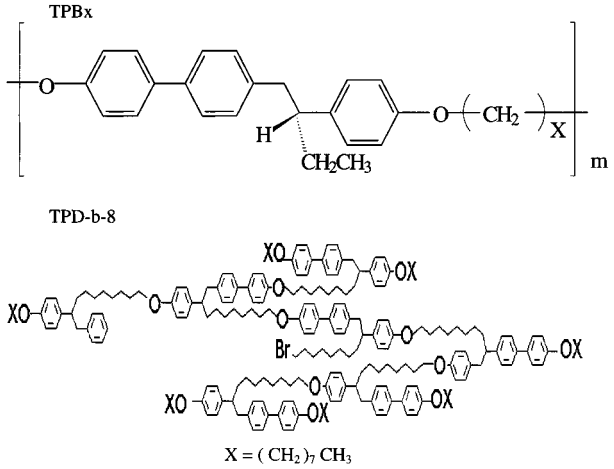

Figure 1. Chemical structure of main-chain LCP TPB*x* and hyperbranched TPD-b-8.

Experimental Section

Materials. Two series of LCPs were investigated in this study: a main-chain LCP, designated TPB*x*, which has a mesogenic group, 1-(4-hydroxy-4′-biphenyl)-2-(4-hydroxyphenyl)butane, separated by flexible alkyl spacers of variable length *x*; and a hyperbranched LCP, designated TPD-b-8, which is based on the mesogen 10-bromo-1-(4-hydroxy-4′-biphenyl)-2-(4-hydroxyphenyl)decane, with octyl groups in the chain end. These polymers have the molecular structures shown in Figure 1. Details of the synthesis and characterization are given elsewhere.[5,6] The nematic solvents used in this study were 4′-(pentyloxy)-4-cyanobiphenyl (5OCB, $T_{NI} = 67$ °C), 4′-pentyl-4-cyanobiphenyl (5CB, $T_{NI} = 35$ °C), 4′-octyl-4-cyanobiphenyl (8CB, $T_{NI} = 40$ °C), and *n*-(*p*-methoxybenzylidene)-*p*′-butylaniline (MBBA, $T_{NI} = 40$ °C). Except for 5CB, these materials were purchased from Aldrich Chemical Co. 5CB was obtained from BDH Ltd. All materials were used as received without further purification.

Methods. (a) Solution Preparation. A specified weight percentage of LCP was dissolved in the nematic solvent (5OCB

[⊗] Abstract published in *Advance ACS Abstracts,* March 1, 1997.

S0024-9297(96)01296-X CCC: $14.00

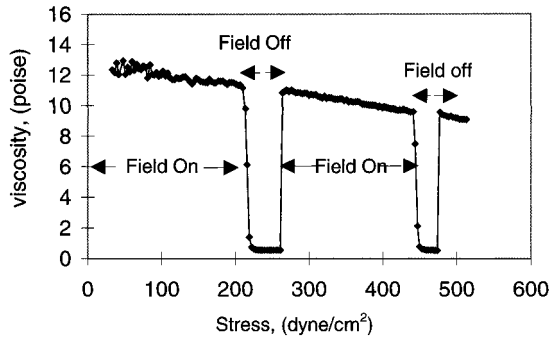

Figure 2. Effect of an applied electric field on the apparent viscosity of a nematic solution of TPB9 ($M_w = 5.58 \times 10^4$) in 5CB at 23.3 °C.

or 5CB) at a temperature above its clearing temperature. Equilibration was continued (requiring at least 24 h) until no visible colloid could be seen in the isotropic solution.

Using a micropipet, nematic samples were placed on the plate of the rheometer, preequilibrated at a selected temperature. The sample quantity was approximately 35 μL. Particular care was taken to ensure that the solution totally filled the gap between the cone and plate and that no air bubbles were present in the sample.

(b) Rheological Analysis. Viscometric measurements were made using a Carrimed controlled-stress rheometer equipped with an attachment that permits application of a dc electric field across the gap, i.e., in the direction perpendicular to the direction of shear. Cone-and-plate geometry was used, with a cone angle of 0.5° and diameter 2 cm, and so the sample is subjected to uniform strain in the radial direction. However, the magnitude of the electric field varies radially, being largest at the tip and smallest at the rim. Using the conductance of the cone and plate, the gap can be set very precisely. For nematic samples, we find that the measured viscosity viscosity at a specified shear stress increases strongly with increasing applied voltage and levels off at 100 V. At this voltage, with a gap at the tip of 15 μm, the average value of the applied field is 2.2 kV/mm. Below this saturation field, the apparent viscosity shows a pronounced decrease with shear stress; above this field, the apparent viscosity is weakly dependent on the applied field and decreases slowly with shear stress. Also in the presence of a saturation field, there is no difference in the measured viscosity if we impose homeotropic alignment on the sample by coating the cone and plate surfaces with lecithin. We also find that the viscosity is reversibly dependent on shear stress in a shear sweep experiment. The sample temperature is controlled to within ±0.1 °C by a water pump circulation system within a temperature range from room temperature to about 90 °C. Before measurements, the samples were maintained under isothermal conditions for 10 min to ensure uniform temperature throughout the gap.

To assess the accuracy of the instrument, we measured the viscosities of standard silicone oils. In the range of 1−10 P, the precision of the measured values is within ±5% error. Below this, the error increases to approximately ±30% for the 0.1 P standard oil.

In measuring the viscosities of low molar mass nematic liquids, we find a significant electrorheological (ER) effect, which becomes particularly large on dissolution of a main-chain LCP. This is illustrated in Figure 2, which shows the effect of an applied field (2.2 kV/mm) on the viscosity measured during a stress sweep for a 2% (w/v) solution of TPB9 ($M_w = 5.58 \times 10^4$) dissolved in 5CB at 23.3 °C. Evidently, the viscosity with the field on is about an order of magnitude larger than that with the field off. Two additional features of this experiment are noteworthy. First, the viscosity decreases approximately linearly with increasing shear stress. This is expected since, with increasing stress, one expects[7] rotation of the director according to the balance of viscous and electric forces:

$$\sigma = \epsilon_0 \epsilon_a E^2 \sin 2\theta / 8\pi \qquad (1)$$

Table 1. Miesowicz Viscosities η_c and η_b of Nematic Solvents

5OCB			5CB			8CB		
T (°C)	η_c	η_b	T (°C)	η_c	η_b	T (°C)	η_c	η_b
52	0.720	0.156	23.3	1.272	0.247	35	0.758	0.282
57	0.523	0.143	27.3	1.007	0.230	37	0.613	0.178
62	0.362	0.130	32.3	0.783	0.212	39	0.524	0.164

Table 2. Concentration Dependence of η_c of TPB9 in 5CB

	% TPB9/5CB (w/v)					
T (°C)	0	0.46	0.75	1.5	2	3
23.3	1.272	2.185	4.290	7.992	12.57	32.83
27.3	1.007	1.819	3.399	5.834	10.06	21.48
32.3	0.783	1.173	2.021	3.604	5.258	14.31

where σ is the shear stress, ϵ_0 is the dielectric permittivity of a vacuum, ϵ_a is the dielectric anisotropy of the nematic solvent, E is the applied electric field strength, and θ is the angle between the nematic director and the electric field direction. For an applied voltage of 100 V, with a tip gap of 15 μm and cone angle of 0.5°, we find the average value of the applied field to be 2.2×10^6 V/m. For 5CB, which has $\epsilon_a = 10$, at shear stress of 100 dyn/cm^2, eq 1 indicates $\theta = 18°$, i.e., that there should be significant rotation of the director and, hence, measurable shear thinning at sufficiently high shear stress, consistent with the experimental observations. Figure 2 also indicates that, at smaller stresses, the noise level of the signal increases because of the limitations of instrumental sensitivity, and so the data obtained below shear rate 15 (1/s) are less reliable. Because of these effects, we use the stress sweep method to measure the apparent viscosity of nematic solutions and extrapolate to zero shear stress to obtain the Miesowicz viscosity η_c.

Results and Discussion

Viscosities of Nematic Solvents. The electrorheological behaviors of four nematic solvents were examined, viz., 5CB, 8CB, 5OCB, and MBBA. 5CB and 5OCB show a small ER effect, and by extrapolation to zero shear under a saturation field, we find that the measured viscosities with the field on and off are numerically close, respectively, to literature values for the Miesowicz viscosities η_c and η_b. This gives us confidence that the electrorheological method will furnish accurate values for the corresponding viscosities of LCP solutions, though we note that the values of η_b are close to the limit of sensitivity of the Carrimed. MBBA has a negative dielectric anisotropy and does not show an electrorheological effect since the electric field rotates the director in the direction of shear. In the nematic state, 8CB also shows a significant ER effect. However, below the transition temperature from nematic to smectic A (33 °C), we find that the viscosity in the presence of the field becomes smaller than that in the absence of the field. We speculate that, with the field on, the smectic alignment is maintained perpendicular to the shear direction, and we measure the small viscosity associated with sliding displacements of the smectic layers. Experimental values of the Miesowicz viscosities η_c and η_b of the nematic solvents at different temperatures are listed in Table 1.

Viscosities of LCP Solutions. (a) Concentration Dependence of η_c and η_b of TPB9 in 5CB. The Miesowicz viscosities η_c and η_b of TPB9 in 5CB were determined over the concentration range 0−3.0% (w/v). The results are tabulated, respectively, in Tables 2 and 3 and plotted in Figures 3 and 4. We find that, below 1.5% (w/v), the viscosity increase is linearly additive. Above 1.5% (w/v), the viscosity increases more strongly with LCP concentration. At a concentration

Table 3. Concentration Dependence of η_b of TPB9 in 5CB

	% TPB9/5CB (w/v)					
T (°C)	0	0.46	0.75	1.5	2	3
23.3	0.247	0.287	0.321	0.396	0.457	0.799
27.3	0.230	0.261	0.303	0.368	0.430	0.774
32.3	0.212	0.236	0.275	0.335	0.395	0.714

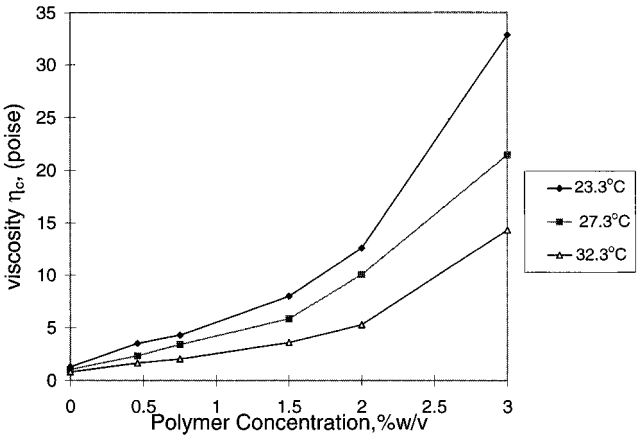

Figure 3. Concentration dependence of Miesowicz viscosity η_c of a nematic solution of TPB9 ($M_w = 5.58 \times 10^4$) in 5CB at 23.3, 27.3, and 32.3 °C.

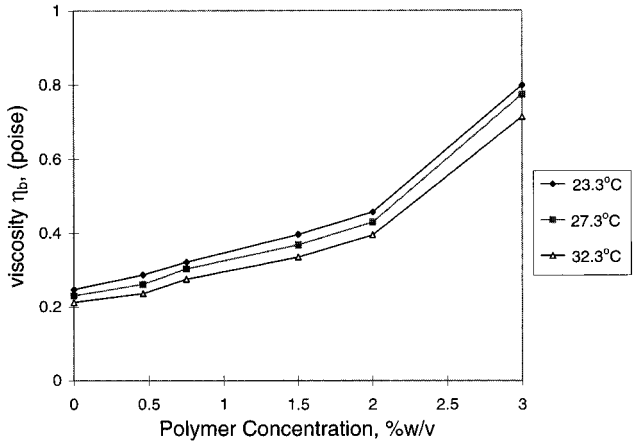

Figure 4. Concentration dependence of Miesowicz viscosity η_b of a nematic solution of TPB9 ($M_w = 5.58 \times 10^4$) in 5CB at 23.3, 27.3, and 32.3 °C.

of 3% (w/v), the stress−strain response shows an apparent yield stress, and the viscosity becomes highly non-Newtonian. In the linear low-concentration regime, we assume that the increments in viscosity can be interpreted by the theoretical analysis of Brochard,[4] as discussed later. Since the concentration dependence of η_c is linear, we present the data in the form of intrinsic viscosity values $[\eta_c] = \lim_{c\to 0}\delta\eta/\eta_c{}^\circ c \cong \delta\eta/\eta_c{}^\circ c$.

(b) Molecular Weight Dependence of $[\eta_c]$ of TPB10 in 5OCB. The molecular weight dependence of the intrinsic Miesowicz viscosity $[\eta_c]$ of TPB10 in 5CB was investigated for four TPB10 samples of different molecular weights. The molecular weights and chain contour lengths of these specimens are listed in Table 4. The true molecular weights, M_w, of TPB10 oligomers are different from the GPC determined values, relative to the polystyrene standards, by a nearly constant ratio.[8] We use this ratio to obtain the true molecular weights for the polymeric species from their GPC molecular weights. Since the density of 5OCB is not known, we specify concentration in units g/g. The least-squares fit to the Mark−Houwink−Sakurada equation at T = 52 °C is shown in Figure 5. The results,

Table 4. Molecular Weights and Chain Contour Lengths of TPB10 Polymers

	tetramer	no. 5	no. 7	no. 8	no. 9
M_c	1966				
$M_{w,GPC}{}^a$	3070	13 330	25 080	45 820	75 440
$M_w/M_n{}^a$	1.0	1.18	1.20	1.28	1.34
$M_w{}^b$	1966	8440	15 860	28 990	47 730
$L_w{}^c$	14.93	62.99	118.15	215.66	354.86

[a] Determined by GPC using chloroform as a solvent and polystyrene as a standard. [b] True molecular weight obtained by correcting $M_{w,GPC}$ via the ratio between $M_{w,GPC}$ and M_c of oligomers. [c] Chain contour length in nanometers based on $M_w{}^b$; $L_w = 4.76n - 1.37(n-1)$, where n is the degree of polymerization, 4.76 nm is the monomer length, 1.37 nm is the extended spacer length.

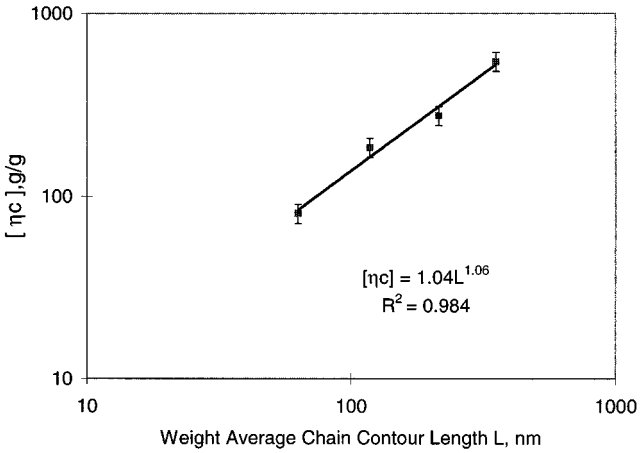

Figure 5. Dependence of the intrinsic Miesowicz viscosity $[\eta_c]$ on chain contour length of TPB10 in 5OCB at 52 °C.

expressed in terms of the true chain contour length L at T = 52, 57, and 62 °C, are

$$\text{at 52 °C} \qquad [\eta_c] = 1.04L^{1.06} \tag{2a}$$

$$\text{at 57 °C} \qquad [\eta_c] = 1.29L^{1.02} \tag{2b}$$

$$\text{at 62 °C} \qquad [\eta_c] = 2.12L^{0.92} \tag{2c}$$

The exponent is evidently very close to unity. Note that the uncertainty in the preexponent is quite large, comparable to its magnitude, in view of the small number of samples. These results can be interpreted within the formalism of the Brochard model.[4] For a chain in an anisotropic solvent, the increment of η_c can be expressed by[4]

$$\delta\eta_c = (CN_A kT/M)(R_{||}{}^2/R_\perp{}^2)\tau_R \tag{3}$$

where C is polymer concentration, k is the Boltzmann constant, T is absolute temperature, $R_{||}$ and $R_\perp$ are the rms end-to-end distances parallel and perpendicular to the director, respectively, and τ_R is the configurational relaxation time, which can be expressed in terms of $\lambda_{||}$ and $\lambda_\perp$, the frictional coefficients parallel and perpendicular to the director:

$$\tau_R = (1/kT)[(\lambda_{||}\lambda_\perp R_{||}{}^2 R_\perp{}^2)/(\lambda_{||}R_{||}{}^2 + \lambda_\perp R_\perp{}^2)] \tag{4}$$

When $R_{||} \gg R_\perp$, eq 3 can be simplified to

$$\delta\eta_c \approx (CN_A kT/M)R_{||}{}^2\lambda_\perp \tag{5}$$

For a Gaussian chain, $R_{||}{}^2 \approx M$, and assuming free draining behavior, $\lambda_\perp \approx M$, whence eq 5 predicts an

Table 5. Miesowicz Viscosity η_c of TPB*x* and TPD-b-8/5OCB Series

	5OCB	TPB5	TPB7	TPB8	TPB9	TPB10	TPD-b-8
M_w		2.82×10^4	3.13×10^4	3.59×10^4	5.58×10^4	4.859×10^4	2.054×10^4
M_w/M_n		1.83	1.91	1.83	1.79	1.82	2.6
% (w/v)		1	1	1	1	1	1.5
				η_c Values			
$\Delta T = 15$ °C[a,b]	0.720 (0.710)	2.05	1.71 (2.35)	3.05 (4.25)	3.95 (3.84)	3.38 (4.99)	1.14
$\Delta T = 10$ °C[a,b]	0.523 (0.533)	1.49	1.33 (1.56)	1.96 (2.68)	2.26 (2.54)	2.33 (3.11)	0.97
$\Delta T = 5$ °C[a,b]	0.362 (0.385)	1.15	1.05 (1.05)	1.51 (1.52)	(1.64)	1.70 (1.96)	0.74 (0.563)
$\Delta T = 0$ °C[b]	0.253		0.73	0.92	1.325		

[a] Data in parentheses are from dynamic light scattering analysis (ref 9). [b] $\Delta T = T_{NI} - T$.

Table 6. Miesowicz Viscosity η_b of TPB*x* and TPD-b-8/5OCB Series

	5OCB	TPB5	TPB7	TPB8	TPB9	TPB10	TPD-b-8
M_w		2.82×10^4	3.13×10^4	3.59×10^4	5.58×10^4	4.859×10^4	2.054×10^4
M_w/M_n		1.83	1.91	1.83	1.79	1.82	2.6
% (w/v)		1	1	1	1	1	1.5
				η_b Values			
$\Delta T = 15$ °C[a,b]	0.156 (0.130)	0.229	0.215 (0.203)	0.254 (0.176)	0.270 (0.178)	0.227 (0.182)	0.250
$\Delta T = 10$ °C[a,b]	0.143 (0.110)	0.214	0.202 (0.165)	0.235 (0.145)	0.229 (0.147)	0.213 (0.148)	0.228
$\Delta T = 5$ °C[a,b]	0.130 (0.091)	0.205	0.184 (0.138)	0.200 (0.113)	(0.127)	0.201 (0.124)	0.213
$\Delta T = -5$ °C[b]	0.117		0.197	0.176	0.1845		0.156

[a] Data in parentheses are from dynamic light scattering analysis (ref 9). [b] $\Delta T = T_{NI} - T$.

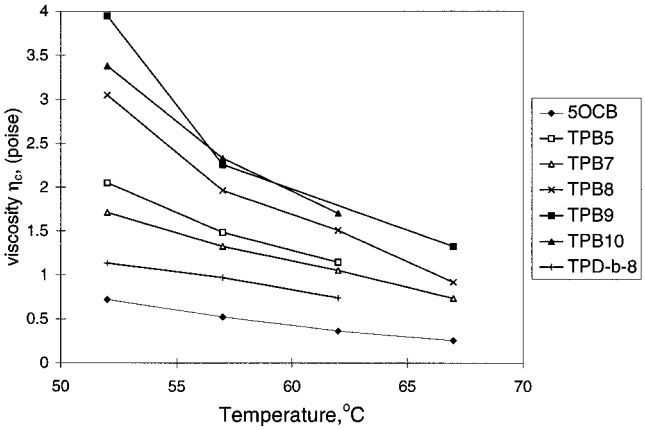

Figure 6. Temperature dependence of Miesowicz viscosity η_c of TPB*x* and TPD-b-8 in 5OCB.

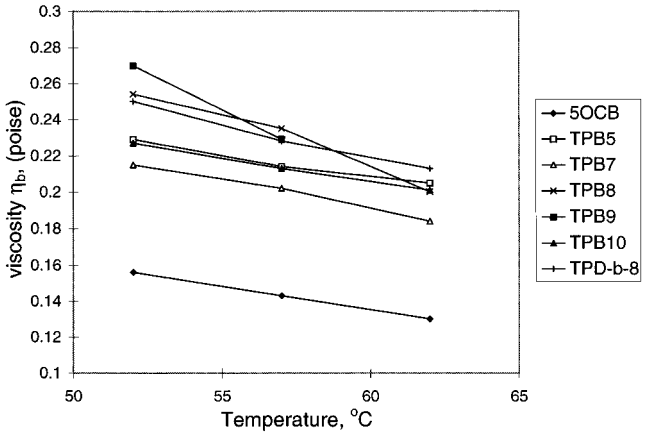

Figure 7. Temperature dependence of Miesowicz viscosity η_b of TPB*x* and TPD-b-8 in 5OCB.

exponent of 1, in agreement with the experimental result. This result is further consistent with our earlier dynamic light scattering measurements[9] of the intrinsic twist viscosity, $[\gamma_1]$, which were obtained at 52 °C:

$$[\gamma_1] = 0.387L^{0.93} \tag{6}$$

(c) Configurational Anisotropy of TPB*x* and TPD-b-8/5OCB. The Miesowicz viscosities η_c and η_b of a series of TPB*x* polymers, differing in spacer length and molecular weight, were measured in 5OCB and are compared with those of a hyperbranched LCP, TPD-b-8, in Tables 5 and 6, respectively. Figures 6 and 7 show the temperature dependence of the Miesowicz viscosities η_c and η_b of the solvent 5OCB and the LCP solutions. The increase in η_c of the TPB*x* solutions over the solvent is large in comparison to that of TPD-b-8. In contrast, the increase in η_b is small and of comparable magnitude for both TPB*x* and TPD-b-8. It should be noted that the Miesowicz viscosity values determined by the present electrorheological method are numerically quite consistent with earlier results extracted indirectly from dynamic light scattering analysis, as demonstrated in Tables 5 and 6. It can be seen that the Miesowicz viscosities η_c from both methods are in very good agreement, whereas the η_b values from the electrorheology method are slightly larger than those from dynamic light scattering. Recall, however, that the present technique measures a viscosity which is close to, but not precisely, η_b.

These results can be further analyzed using the Brochard theory[4] to generate information on the configurational anisotropy of the LCP in nematic solution. This is possible by combining eq 3 for $\delta\eta_c$ with the corresponding equation for $\delta\eta_b$:

$$\delta\eta_b = (CN_A kT/M)(R_\perp^2/R_\parallel^2)\tau_R \tag{7}$$

Dividing eq 3 by eq 7, we obtain

$$\delta\eta_c/\delta\eta_b = R_\parallel^4/R_\perp^4 \tag{8}$$

which indicates that we can determine the chain anisotropy ratio $R_\parallel/R_\perp$ directly by taking the ratio of the viscosity increments. Since the measured viscosity with the field off will be slightly larger than the true η_b, the experimental chain anisotropies will underestimate the correct values. Note that eq 8 provides a molecular rationale for the large ER effect exhibited by solutions of main-chain LCPs in low molar mass nematic solvents which have positive dielectric anisotropies.

Table 7. Chain Anisotropy of LCPs in 5OCB

	$R_\parallel/R_\perp$					
T (ΔT) (°C)	TPB5	TPB7	TPB8	TPB9	TPB10	TPD-b-8
52 (15)	2.065	2.025	2.207	2.307	2.473	1.450
57 (10)	1.919	1.921	1.989	2.119	2.254	1.514
62 (5)	1.798	1.890	2.011		2.022	1.459

The values of $R_\parallel/R_\perp$ of TPB*x* and TPD-b-8 in 5OCB obtained via eq 8 at different temperatures in the nematic region are listed in Table 7. The results indicate that the chain anisotropy of TPB*x* is large ($R_\parallel/R_\perp \approx 1.8-2.5$) in comparison to that of TPD-b-8 ($R_\parallel/R_\perp \approx 1.5$). Also, the anisotropy for TPB*x* shows a decreasing trend with increasing temperature, whereas that of TPD-b-8 is essentially independent of temperature. Clearly, these observations are consistent with the hyperbranched structure of TPD-b-8 (Figure 1).

Conclusions

We have measured the increments in Miesowicz viscosities $\delta\eta_c$ and $\delta\eta_b$ on dissolving liquid crystal polymers in nematic solvents by the electrorheological method. In very dilute solution, the viscosities increase linearly with LCP concentration, consistent with a theoretical description by Brochard. A pronounced electrorheological effect is observed for the main-chain LCP TPB*x*, reflecting the fact that, in the presence of an applied field, the configurationally anisotropic chains align in the nematic solvent perpendicular to the flow direction, leading to a large increase in viscosity ($\delta\eta_c$). In the absence of the field, the chains align with the flow field, yielding a small increase in viscosity ($\delta\eta_b$). The intrinsic viscosity, $[\eta_c]$, shows a strong dependence on chain contour length, $[\eta_c] \approx L^{1.0}$, consistent with behavior predicted for a biased free-draining Gaussian chain via the Brochard model. Finally, analysis of the viscosity increments $\delta\eta_c$ and $\delta\eta_b$ for the hyperbranched LCP TPD-b-8, using the Brochard model, is consistent with the expectation that it has a smaller chain anisotropy in the nematic state than the main-chain LCP.

Acknowledgment. We thank Dr. Fu-Lung Chen for useful advice. Also, financial assistance from NSF Materials Research Group Award DMR 01845 and NSF Science and Technology Center ALCOM DMR 89-20147 is gratefully acknowledged.

References and Notes

(1) (1) Skarp, K.; Lagerwall, S. T.; Stebler, B. *Mol. Cryst. Liq. Cryst.* **1980**, *60*, 215.
(2) Yang, I. K.; Shine, A. D. *J. Rheol.* **1992**, *36*, 1079.
(3) Tse, K. L.; Shine, A. D. *J. Rheol.* **1995**, *39*, 1021.
(4) Brochard, F. *J. Polym. Sci.: Polym. Phys. Ed.* **1979**, *17*, 1367.
(5) Percec, V.; Kawasumi, M. *Macromolecules* **1991**, *24*, 6318.
(6) Percec, V.; Kawasumi, M. *Macromolecules* **1992**, *25*, 3843.
(7) Gennes, P. G.; Prost, J. *The Physics of Liquid Crystals*, 2nd ed.; Clarendon Press: Oxford, 1993; pp 134, 210.
(8) Kawasumi, M. Ph.D. Thesis, Department of Macromolecular Science, Case Western Reserve University, Cleveland, OH, 1993.
(9) Chen, F. L.; Jamieson, A. M. *Macromolecules* **1994**, *27*, 1943.

MA961296P